

Towards Generalizable Deepfake Detection with Spatial-Frequency Collaborative Learning and Hierarchical Cross-Modal Fusion

Mengyu Qiao*
North China University of
Technology
Beijing, China
myuqiao@ncut.edu.cn

Runze Tian
North China University of
Technology
Beijing, China
trz@mail.ncut.edu.cn

Yang Wang
Ultramain Systems, Inc.
Albuquerque, NM, USA
ywang@ultramain.com

Abstract

The rapid evolution of deep generative models poses a critical challenge to deepfake detection, as detectors trained on forgery-specific artifacts often suffer significant performance degradation when encountering unseen forgeries. While existing methods predominantly rely on spatial domain analysis, frequency domain operations are primarily limited to feature-level augmentation, leaving frequency-native artifacts and spatial-frequency interactions insufficiently exploited. To address this limitation, we propose a novel detection framework that integrates multi-scale spatial-frequency analysis for universal deepfake detection. Our framework comprises three key components: (1) a local spectral feature extraction pipeline that combines block-wise discrete cosine transform with cascaded multi-scale convolutions to capture subtle spectral artifacts; (2) a global spectral feature extraction pipeline utilizing scale-invariant differential accumulation to identify holistic forgery distribution patterns; and (3) a multi-stage cross-modal fusion mechanism that incorporates shallow-layer attention enhancement and deep-layer dynamic modulation to model spatial-frequency interactions. Extensive evaluations on widely adopted benchmarks demonstrate that our method outperforms state-of-the-art deepfake detection methods in both accuracy and generalizability.

CCS Concepts

• **Computing methodologies** → **Computer vision representations**; • **Information systems** → **Multimedia and multimodal retrieval**.

Keywords

Deepfake Detection, Discrete Cosine Transform, Cross-Modal Fusion, Spatial-Frequency Learning, Convolutional Neural Network

1 Introduction

The rapid advancement of deep-generative models [4][19][20] has catalyzed the evolution of facial manipulation techniques, enabling the creation of highly realistic synthetic media (commonly termed "deepfakes"). Although these technologies [7][17][23][39] enable potential applications in the entertainment and creative industries, their misuse poses significant social risks, including disinformation propagation, identity theft, and political fraud. Consequently, detecting deepfake content has emerged as a critical challenge in multimedia security and computer vision.

Most existing deepfake detection methods [24][38][8][1] formulate the task as binary classification, where backbone networks are typically used to extract discriminative features. Analysis and detection [49][41][33][46][48] predominantly focus on artifacts in the spatial domain, such as facial inconsistencies, unnatural textures, blending boundaries, etc. However, as sophisticated deepfake techniques increasingly refine spatial details, the distinctions between authentic and forged faces at the pixel level have become remarkably subtle and undetectable. This limitation reveals the inherent vulnerability of spatial domain approaches, particularly when confronting high-quality forgeries or post-processing perturbations.

In contrast, frequency domain analysis offers a complementary perspective for uncovering manipulation traces. Forged faces often exhibit distinctive spectral patterns, such as inconsistencies in high-frequency noise or anomalies introduced by upsampling operations in generative models. Despite this potential, existing frequency-aware methods [43][2][37][22][29] typically augment spatial anomalies through intermediate filtering operations in spectral representations and finalize feature extraction in spatial domain, neglecting the intrinsic abnormal patterns manifested across frequency sub-bands, especially in the local forged regions, as shown in Figure 1. Although several works [35][21] incorporate block-wise frequency transformations, they fail to deeply investigate the interdependencies among frequency features. Furthermore, most methods inadequately address the dependence between image semantics and forgery artifacts, resulting in limited generalization across datasets and manipulation types.

To address these challenges, we propose a Spatial-Frequency Collaborative Learning (SFCL) framework that simultaneously extracts features from both spatial and frequency domains while enabling multi-stage feature interaction through a Hierarchical Cross-Modal Fusion (HCMF) mechanism. For frequency domain processing, we depart from conventional global frequency transformation and instead adopt a localized analysis paradigm. Specifically, we employ block-wise Discrete Cosine Transform (DCT) to precisely capture frequency domain artifacts while retaining macro-level spatial semantics. To model the distribution pattern of intra-block DCT coefficients and the transitional patterns of inter-block DCT sub-bands, we construct a local branch in the frequency pipeline that extracts multi-scale frequency features through cross-band and cross-block convolution. Additionally, we introduce a global branch in the frequency pipeline, to compute statistical frequency features from horizontal and vertical derivatives of DCT sub-bands across blocks of a face patch at the original resolution. Finally, we incorporate

*Corresponding author.

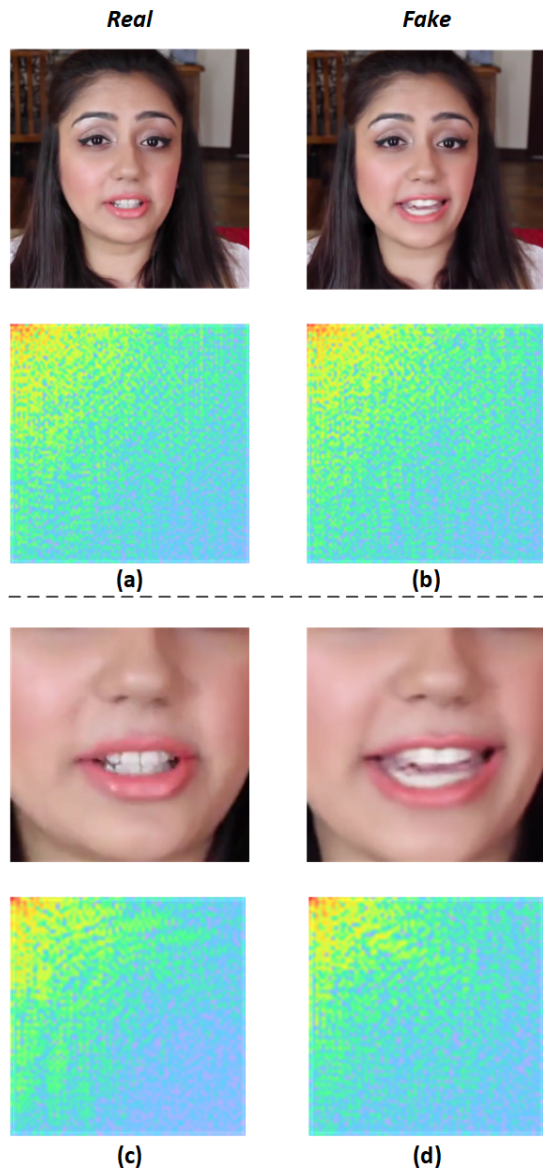


Figure 1: (a) (b) represent heatmaps of Full-Image DCT transform and (c) (d) represent heatmaps of Local Regional DCT Transform between real and fake images.

a frequency-guided attention mechanism to enhance spatial features in the shallow layers of the network while enabling effective cross-modal fusion in the deep layers.

Extensive experiments on benchmark datasets (FaceForensics++, Celeb-DF, and DFDC) validate the superior performance of our method in both intra-dataset evaluation and cross-dataset generalization. In summary, the contributions of this study are threefold as below:

- We propose a novel block-wise discrete cosine transform analysis approach with inter/intra-block multi-scale frequency-convolutional network. Through progressive feature abstraction in the DCT transform domain, this approach effectively captures both intra-block spectral characteristics and inter-block transitional patterns, thereby enhancing local representation learning and precise artifact modeling in the frequency domain.
- We propose a global spectral feature extraction and synthesis approach based on scale-invariant differential analysis. This approach models holistic forgery patterns across regions of interest while minimizing multi-scale discrepancies and reducing interference from post-processing operations.
- We develop a hierarchical cross-modal fusion mechanism that integrates shallow-layer attention enhancement and deep-layer dynamic modulation. This design effectively models spatial-frequency interactions, addresses modality-specific feature heterogeneity in detection tasks, and maintains robustness against sophisticated forgery manipulations.

2 Related Works

Early detection methods focused on the unnatural biological signals in forgeries, such as abnormal mouth movements during speech [3], head poses [45], irregular blink frequency and anomalies in remote visual photoplethysmography (rPPG) [9][18][34][15].

With the advancement of deep learning, various models [8][38][1] have been widely adopted as backbone networks to detect deepfake in the spatial domain. To further improve performance, many methods [49][42][5][32] incorporate specialized functional modules to enhance the learning of localized forgery patterns. For instance, M2TR [40] and HFI-Net [31] leverage the complementary strengths of Vision Transformers (ViTs) [12] and convolutional neural networks (CNNs) to boost detection accuracy. MAD [49] introduces a multi-attentional architecture equipped with texture enhancement blocks and a regional independence loss, allowing the network to attend to non-overlapping regions and capture fine-grained local forgery cues. Nirkin et al. [33] propose a method that exploits discrepancies between facial regions and their surrounding context, based on the observation that most manipulation techniques modify only the face while preserving peripheral features such as hair, ears, and neck. Additionally, some approaches detect manipulations by integrating noise features [47][41][29][50] with RGB features.

Recent studies [13][35][22][30][28][16][27] reveal the promising effects of discriminative patterns in the frequency domain for deepfake detection. Qian et al. [35] proposed F3-Net, separating frequency components via DCT and fusing local frequency statistics, achieving robustness on compressed videos. Durall et al. [13] analyzed high-frequency spectral anomalies using Discrete Fourier Transform (DFT), providing theoretical insights into frequency-domain forgery patterns. Several approaches leverage the complementarity between the frequency domain and RGB features. Masi et al. [30] designed a dual-stream network combining Laplacian-of-Gaussian frequency enhancements with spatial features. Liu et al. [28] jointly modeled upsampling artifacts using phase spectra and spatial frequency relation [42][31][16][14] was studied to leverage the representational capacity of multi-modal

learning. Although these methods utilize frequency analysis, most of them simply rely on filter-based approaches to enhance spatial domain detection, lack in-depth exploration of diverse frequency characteristics at local and global scales, and neglect the interactions of the spatial and frequency domains at different stages.

3 Methods

3.1 Overview

This section presents the design motivations and architectural overview of our proposed framework. Modern deepfake techniques progressively synthesize content from local to global scales, often resulting in inter-block pattern inconsistencies, particularly around semantic boundaries, such as facial regions. To address diverse patterns of deepfake artifacts, we employ a Spatial-Frequency Collaborative Learning paradigm to achieve comprehensive representation and generalizable detection. An overview of our proposed framework is illustrated in Figure 2.

In the frequency domain, deepfake manipulations tend to introduce additive noise or unnatural spectral distortion during the synthesis of fine-grained details. We hypothesize that applying block-wise DCT transform enables direct analysis of high-, mid-, and low-frequency artifacts within each local patch. By partitioning images into blocks, our method focuses on localized spectral characteristics, thereby mitigating the detail loss inherent in global transformations while enhancing sensitivity to subtle anomalies.

We identify the limitations of popular backbone network architectures in frequency domain analysis. Specifically, standard 2D-CNN backbones are insufficient for capturing deep interdependencies among DCT coefficient distributions within image blocks and lack the representational capacity for effective inter-block frequency analysis. Moreover, many existing methods rely on upsampling or downsampling operations (e.g., sinc or bilinear interpolation) to align input dimensions, which often degrades frequency-domain artifacts and diminishes discriminative performance.

Motivated by these observations, we propose a Local-Global Frequency Framework within the frequency analysis pipeline. This framework integrates two complementary branches: Local Branch: We design an inter/intra-block multi-scale frequency-convolutional network to hierarchically model intra-block spectral coefficient correlations and inter-block transitional patterns, enabling localized frequency feature extraction. Global Branch: We introduce Scale-Invariant Differential Analysis (SIDA), applied to cropped regions of interest in original resolution. This approach avoids high-frequency degradation caused by resampling and preserves scale-invariant spectral fingerprints critical for global pattern analysis.

Moreover, we also incorporate a spatial domain analysis pipeline by utilizing an EfficientNet backbone network which is pre-trained on image classification tasks and fine-tuned on deepfake detection tasks to capture local spatial artifacts, such as textures, edges, and structural inconsistencies.

To bridge the frequency and spatial domains, we further propose a Hierarchical Cross-Modal Fusion Framework. In the shallow layers, we incorporate a Frequency-Aware Attention Enhancement Module (FAAE), which generates block-wise, frequency-localized

attention maps from spectral features. This enhances spatial representations by highlighting localized forgery cues. In the deeper layers, we implement a Hybrid Cross-Modal Attention Fusion Module, which combines hybrid attention mechanisms for spatial-frequency coherence with differential-enhanced gating for anomaly amplification. Together, these modules enable the effective integration of multi-modal representations through hierarchical interactions.

3.2 Local-Global Frequency Framework

Formally, let the input image be denoted as $X \in \mathbb{R}^{C \times H \times W}$, where H and W represent the height and width, respectively, and C denotes the number of channels. Following the approach in [44], we first convert the RGB image to the YCbCr color space. Subsequently, block-wise DCT transforms with a block size of 8×8 are applied across all three channels, consistent with standard image compression protocols such as JPEG. Each block of DCT coefficients is then flattened into a one-dimensional vector using zigzag scanning, which orders the coefficients from low to high frequency. This process aligns coefficients corresponding to the same frequency components across channels and systematically organizes all blocks based on their frequency content. The resulting representation is a restructured 4D tensor $\tilde{X} \in \mathbb{R}^{C \times 64 \times H/8 \times W/8}$, which explicitly preserves spatial-frequency relationships crucial for subsequent analysis. As shown in Figure 3.

3.2.1 Global Branch. Conventional preprocessing pipelines typically resize input images to fixed dimensions to facilitate batch processing. However, this operation inevitably alters the spectral energy distribution of forged regions and compromises the integrity of high-frequency information. To address this limitation, the global branch introduces the SIDA module that preserves block-wise DCT transformations at the original resolution while maintaining shape consistency of spectral features across images with varying spatial dimensions. Specifically, we first localize facial regions using a face tracking algorithm to obtain bounding box coordinates, within which block-wise DCT transformations are exclusively performed to retain region-specific spectral information.

For inter-block scale analysis, localized manipulations often cause abrupt variations in frequency distributions between adjacent row and column blocks. To capture transitional inconsistencies, we apply horizontal and vertical differential operations to eliminate semantic information while amplifying manipulation-specific anomalies. We compute inter-block differential operations on the frequency-transformed features \tilde{X} , deriving inter-block row differential features $\tilde{X}_{row} \in \mathbb{R}^{C \times 64 \times (H/8) \times ((W/8)-1)}$ and inter-block column differential features $\tilde{X}_{col} \in \mathbb{R}^{C \times 64 \times ((H/8)-1) \times (W/8)}$, which can be represented by equation 1 and 2.

$$\tilde{X}_{row} = \tilde{X}_{:, :, m+1, :} - \tilde{X}_{:, :, m, :}, m \in [1, (H/8) - 1] \quad (1)$$

$$\tilde{X}_{col} = \tilde{X}_{:, :, :, n+1} - \tilde{X}_{:, :, :, n}, n \in [1, (W/8) - 1] \quad (2)$$

At the intra-block scale, forged regions often display anomalous spectral energy distributions. Intra-block coefficient differentials quantify local correlations between adjacent frequency components. We then perform intra-block differential operations on \tilde{X} to obtain intra-block differential features $\tilde{X}_{intra} \in \mathbb{R}^{C \times 63 \times (H/8) \times (W/8)}$ as represented in equation 3, which then undergoes zero-padding

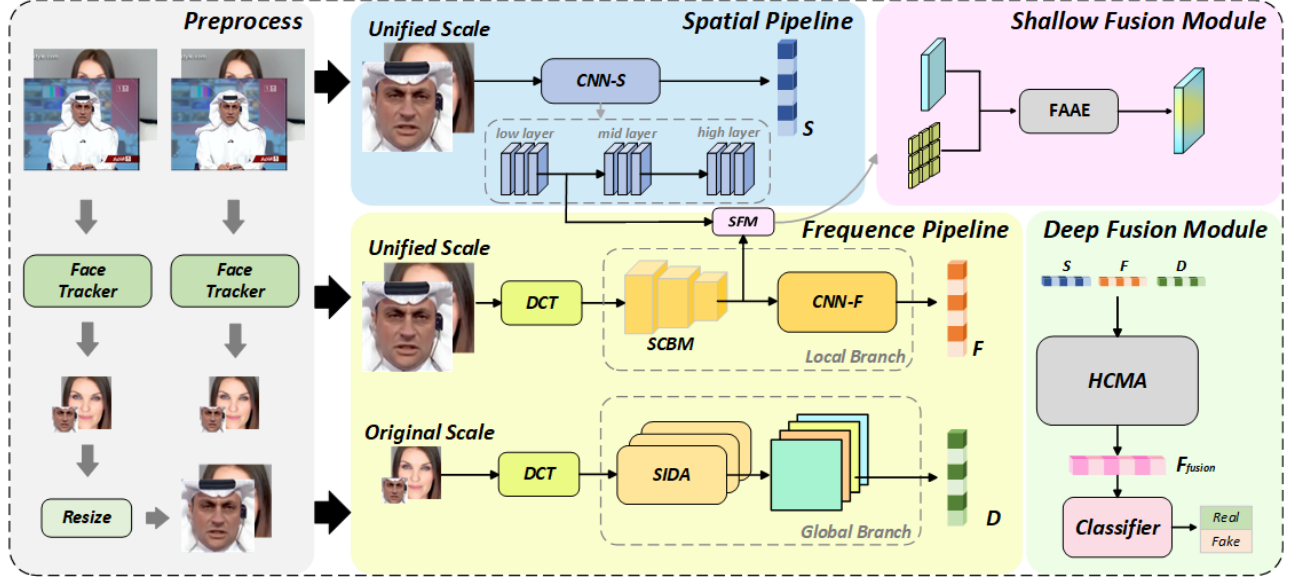


Figure 2: The architecture of SFCL-HCMF.

along the intra-block dimension to maintain dimensional consistency.

$$\tilde{X}_{intra} = \tilde{X}_{:,l+1,:} - \tilde{X}_{:,l,:}, l \in [1, 63] \quad (3)$$

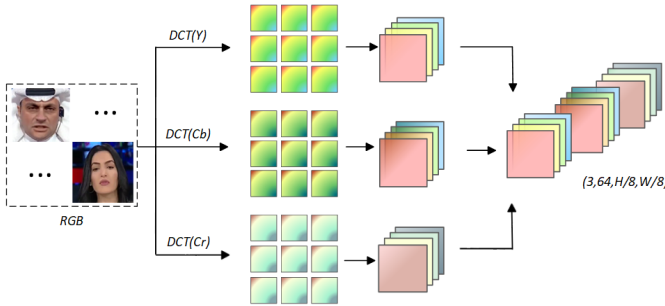


Figure 3: The block-wise DCT transform.

Subsequently, four statistical metrics—mean, std, skewness, and kurtosis, are computed on the absolute values of the three derivative feature maps, as shown in equation 4-7:

$$Mean_k = \frac{1}{H \times W} \sum_{i=1}^H \sum_{j=1}^W |\tilde{X}_k^{i,j}|, (k = row, col, intra) \quad (4)$$

$$Std_k = \sqrt{\frac{1}{H \times W} \sum_{i=1}^H \sum_{j=1}^W (\tilde{X}_k^{i,j} - Mean_k)^2} \quad (5)$$

$$Skew_k = \frac{\frac{1}{H \times W} \sum_{i=1}^H \sum_{j=1}^W (\tilde{X}_k^{i,j} - Mean_k)^3}{Std_k^3} \quad (6)$$

$$Kurt_k = \frac{\frac{1}{H \times W} \sum_{i=1}^H \sum_{j=1}^W (\tilde{X}_k^{i,j} - Mean_k)^4}{Std_k^4} \quad (7)$$

This aggregation process transforms localized discrepancy intensities into global statistical descriptors, thereby capturing holistic distribution patterns of forgery traces rather than relying on position-specific artifacts. Subsequently, the four types of differential statistical features are flattened and concatenated to form a global differential frequency representation $D \in \mathbb{R}^{2304}$ as shown in equation 8, which effectively encodes vertical, horizontal, and intra-spectral anomaly patterns.

$$D = cat(\text{flat}(Mean_k), \text{flat}(Std_k), \text{flat}(Skew_k), \text{flat}(Kurt_k)) \quad (8)$$

3.2.2 Local Branch. 2D CNNs exhibit inherent limitations in processing high-dimensional spectral features, failing to capture cross-frequency correlations (along the channel dimension) within individual image blocks. To address these limitations, we designed **Intra/Inter-block Multi-Scale Frequency-convolutional Network**, which consists of SBCM and CNN-F. The pipeline of Local Branch is depicted in Figure 4.

2D CNNs exhibit inherent limitations in processing high-dimensional spectral features, as they fail to capture cross-frequency correlations (i.e., along the channel dimension) within individual image blocks. To overcome these challenges, we propose an Multi-Scale Frequency-Convolutional Network, which consists of a Spectral Band Convolution Module (SBCM) and a Frequency Convolutional Neural Network (CNN-F).

SBCM. This module employs stacked 3D convolutional blocks with $kernel\ size=(x, 1, 1)$ to capture inter-channel correlations among spectral coefficients. By sliding 3D kernels along the spectral band

dimension, SBCM progressively learns localized interaction patterns across adjacent frequency bands. Initial layers utilize larger kernels to establish long-range dependencies among low-, mid-, and high-frequency components for cross-band feature aggregation; intermediate layers progressively reduce x to focus on abrupt spectral transitions caused by forgery artifacts, enhancing anomaly responses in mid-frequency regions; final layers adopt minimal x to isolate high-frequency noise patterns and magnify distributional irregularities within critical spectral bands.

The processed spectral-semantic features, denoted as $X_f^{local} \in \mathbb{R}^{C \times 3 \times (H/8) \times (W/8)}$, where $C=64$, thereby encapsulate hierarchically refined frequency-specific representation.

We then flatten the first two dimensions of the tensor, differing from the initial direct flattening approach, where each spatial location's 192-dimensional features now encapsulate high-level semantic characteristics with cross-band correlations, as shown in equation 9.

$$X_f^{local} = flat(X_f^{local}, dim = (0, 1)) \quad (9)$$

CNN-F To model the relationships between heterogeneous image blocks, we adapt conventional CNN architectures—exemplified by Xception—through modifications to the input layers. Specifically, we remove the first two convolutional layers and one depthwise separable convolutional block, replacing them with SBCM. To maintain architectural compatibility, we then adjust the input channels of the subsequent depthwise separable convolution block to match the channel dimension of the output spectral features X_f^{local} . This hierarchical processing framework enables the modeling of both intra- and inter-block correlations among DCT coefficients, resulting in frequency-aware features $F \in \mathbb{R}^{2048}$.

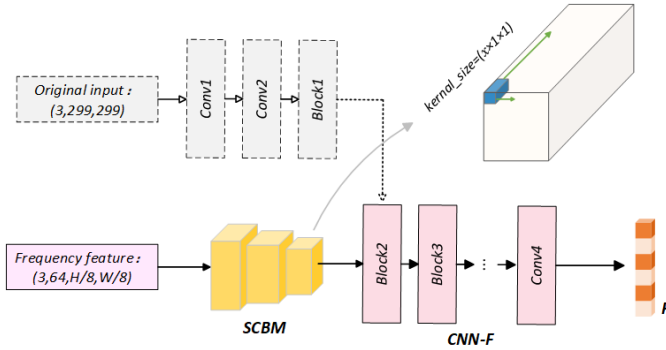


Figure 4: The pipeline of Local Branch (inter/intra-block multi-scale frequency-convolutional network)

3.3 Hierarchical Cross-Modal Fusion

3.3.1 Frequency-Aware Attention Enhancement. We aim to amplify localized forgery artifacts at the shallow layers of the spatial domain model, thereby enhancing the saliency of subtle manipulation traces to foster the learning of discriminative feature representations. The structure of Frequency-Aware Attention Enhancement module is shown in Figure 5.

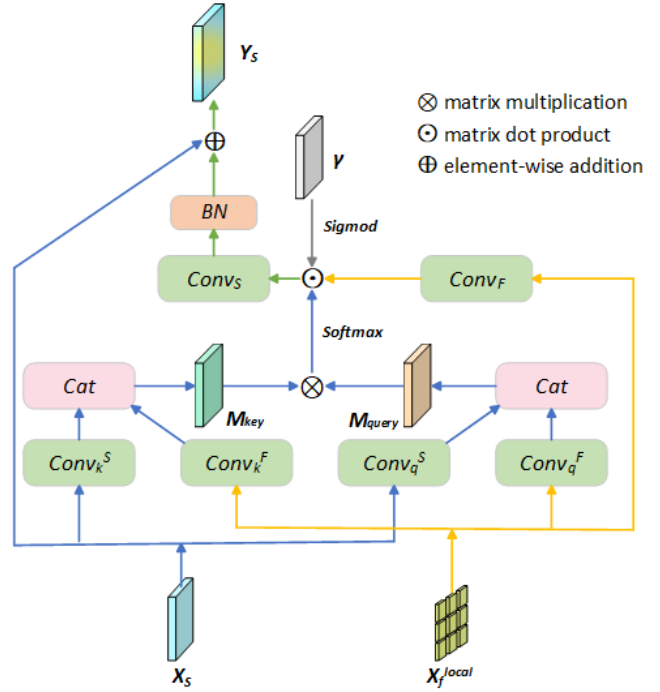


Figure 5: The structure of Frequency-Aware Attention Enhancement module.

The module initially receives two inputs: the shallow-layer spatial features X_S and the spectral features of SBCM's output X_f^{local} . We first generate cross-modal query-key pairs through parallel convolutional projections, while aligning channel dimensions to ensure compatibility, as shown in equation 10 and 11.

$$M_{query} = cat(Conv_q^F(X_f^{local}), Conv_q^S(X_S)) \quad (10)$$

$$M_{key} = cat(Conv_k^F(X_f^{local})^T, Conv_k^S(X_S)^T) \quad (11)$$

The cross-modal attention weight matrix α is subsequently derived through scaled dot-product computation between the concatenated key pairs, which encapsulates the spectral-spatial interaction dynamics by correlating frequency-localized patterns with spatial anomalies, as shown in equation 12.

$$\alpha = Softmax\left(\frac{M_{query}M_{key}^T}{\sqrt{2H}}\right) \quad (12)$$

The spatial refinement branch injects frequency context constraints through attention gating. Here, $Conv_F$ projects spectral-domain features to align with the spatial feature dimensions, γ_S denotes learnable parameters that dynamically regulate the contribution intensity of spectral features to the spatial branch, σ represents the Sigmoid activation function, and $Conv_S$ adapts the dimensionality of the frequency-aware attention matrix to ensure dimensional compatibility during cross-modal feature fusion, as shown in equation 13.

$$Y_S = X_S + BN(Conv_S(\alpha \odot Conv_F(X_f^{local}) \cdot \sigma(\gamma_S))) \quad (13)$$

3.3.2 *Hybrid Cross-Modal Attention Fusion.* To establish deep interactive reasoning between spatial and spectral domains, we propose an HCMA multi-modal fusion module, as is shown in Figure 6. The module first projects spatial deep features $S \in \mathbb{R}^{1792}$ and intra/inter-block frequency correlation features $F \in \mathbb{R}^{2048}$ into a unified embedding space through linear transformation layers $S', F' \in \mathbb{R}^{1792}$, eliminating modality-specific dimensional discrepancies.

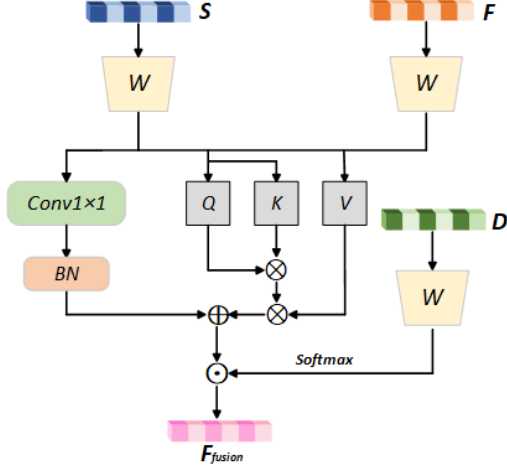


Figure 6: The structure of Hybrid Cross-Modal Attention Fusion.

Using spatial features as Query vectors $Q = S'W_Q$, and frequency features as Key-Value pairs $K = F'W_K, V = F'W_V$, where $W_Q, W_K, W_V \in \mathbb{R}^{1024 \times 1024}$ are learnable parameter matrices. Then, multi-head attention is used to capture cross-modal global dependencies to generate attention-weighted representations, as shown in equation 14.

$$A = \text{softmax}\left(\frac{QK^T}{\sqrt{1024/h}}\right)V \quad (14)$$

To enhance fusion performance, we introduce residual connections by adding the attention output with 1D-convolution-processed spatial features followed by batch normalization, thereby maintaining gradient stability, as shown in equation 15.

$$A_{res} = A + \text{BN}(\text{Conv}_{1 \times 1}(S')) \quad (15)$$

Considering the sensitivity of differential statistical features to manipulated regions, a dynamic gating mechanism is designed—projecting differential frequency statistical representation $D \in \mathbb{R}^{2304}$ into gating coefficients via Sigmoid activation, which modulates features to amplify anomaly responses, as shown in equation 16 and 17.

$$g = \alpha(W_g D + b_g), W_g \in \mathbb{R}^{1024 \times 2304} \quad (16)$$

$$F_{fused} = A_{res} \odot g \quad (17)$$

This architecture achieves hierarchical cross-modal feature synergy, combining global dependency modeling with local anomaly enhancement capabilities. Finally, the fused multi-modal semantic representation vectors are fed into the classifier to execute discriminative decision-making for deepfake detection tasks.

4 Experiments

4.1 Implement Details

For each video clip, we first extract the same amount of frames. Then, we employ the state-of-the-art face detector dlib to record facial bounding box coordinates for each image. During preprocessing, facial regions are cropped based on these coordinates (Face Tracker), and block-wise DCT transform with a block size of 8×8 is applied. The spatial pipeline and local stream of the frequency domain pipeline accepts inputs of 380×380 resolution, while the global stream of the frequency domain pipeline processes data into identical dimensions using the SIDA operations. In the model architecture, we adopt EfficientNet-B4 pre-trained on ImageNet as the backbone for the spatial-domain pipeline. In SCBM, 3D convolutional kernel sizes are set to 7, 5, and 3 sequentially. The HCMA module utilizes multi-head attention with 8 heads. For training, we optimize the model using the Adam optimizer with a learning rate of 0.001, weight decay of $1e-8$, and a batch size of 20. The model is trained for 20 epochs on two NVIDIA RTX 4090 GPUs.

Table 1: In-dataset evaluation results on the FF++ dataset with varying compression levels. The best results are highlighted in bold, and the second-best results are underlined.

Methods	FF++(HQ)		FF++(LQ)	
	Acc(%)	AUC(%)	Acc(%)	AUC(%)
Xception[8]	95.73	96.30	86.86	89.30
X-Ray[24]	-	87.40	-	61.60
Two Branch[30]	-	98.70	-	86.56
SPL[28]	91.50	95.32	81.57	82.82
MAD*[49]	<u>97.17</u>	<u>99.28</u>	87.35	89.92
EDD[11]	96.19	98.81	88.69	<u>91.27</u>
M2TR*[40]	96.73	99.16	<u>89.36</u>	91.08
HFI-Net[31]	95.12	98.66	<u>86.90</u>	90.75
ED[6]	94.98	98.30	-	-
SPCL-HCMF(ours)	97.43	99.58	91.77	94.21

4.2 Datasets

Our experiments are primarily conducted on the FaceForensics++ (FF++) [36] dataset. FF++ comprises 1,000 original videos and 4,000 corresponding manipulated videos generated by four distinct forgery methods: Deepfakes, Face2Face, FaceSwap, and NeuralTextures. The dataset includes three compression levels: c0 (raw/uncompressed), c23 (light compression), and c40 (heavy compression). We focus on the c23 and c40 versions for evaluation.

The Celeb-DF [25] dataset contains two versions (v1 and v2), featuring interviews with 59 celebrities across diverse ages, ethnicities, and genders. The v1 subset includes 409 real videos and 795 synthesized videos, while v2 expands this to 590 real and 5,639 manipulated videos. We conducted cross-dataset evaluation using the enhanced v2 version, which incorporates a broader diversity of manipulation types.

The DFDC (DeepFake Detection Challenge) [10] dataset is a benchmark dataset comprising over 100,000 video clips sourced from 3,426 actors. In our experiments, the DFDC dataset is primarily used to evaluate the cross-dataset generalization capability of our model.

Table 2: Performance comparison of different methods on various datasets. The best results are highlighted in bold, and the second-best results are underlined.

Methods	Years	Training dataset	FF++(c23) AUC(%)	Celeb-DF(v2) AUC(%)	DFDC AUC(%)
Xception[8]	2017	FF++(c23)	96.30	65.30	72.20
Two-branch[30]	2020		93.18	73.41	-
X-Ray[24]	2020		87.40	-	70.00
F ³ -Net[35]	2020		98.10	65.17	-
MAD*[49]	2021		99.28	67.44	65.56
M2TR*[40]	2022		99.16	65.17	-
SFDG[42]	2023		<u>99.53</u>	75.83	<u>73.64</u>
DAW-FDD[26]	2024		98.28	74.42	61.47
SPCL-HCMF(ours)	-		99.58	<u>74.68</u>	73.71

4.3 Evaluation Metrics

We adopt Accuracy (Acc) and Area Under the ROC Curve (AUC) as evaluation metrics, which are standard measures in deepfake detection research. All experimental results are reported at the image level.

4.4 In-dataset evaluation

To evaluate the effectiveness of the proposed method, we first perform intra-dataset experiments on the FaceForensics++ (FF++) dataset. Following the standard protocol, the dataset comprising 1,000 videos is partitioned into 720 for training, 140 for validation, and 140 for testing. For each video, 270 frames are extracted, and a four-fold augmentation is applied to balance the class distribution.

We conduct experiments on both the high-quality (HQ, c23) and low-quality (LQ, c40) compression settings, and report Accuracy (Acc) and Area Under the Curve (AUC) metrics in Table 1. Our approach is benchmarked against state-of-the-art detection methods, including X-Ray [24], MAD [49], and M2TR [40], etc. As shown in the results, our method achieves superior performance under both compression levels. In particular, when compared to frequency-aware baselines such as SPSL [28] and HFI-Net [31], our approach improves detection accuracy by 5.9% and 2.3% on HQ, respectively.

4.5 Cross-dataset evaluation

To demonstrate the generalization capability of our method, we conduct cross-dataset evaluations on multiple benchmark datasets. This setting presents greater challenges due to significant distribution shifts among datasets. Specifically, we train our model on FF++ (HQ) and evaluate it on Celeb-DF (v2) and DFDC. For each video, we extract 50 frames and compute the frame-level AUC scores. As shown in Table 2, our method achieves superior or comparable performance across all cross-dataset evaluations. Notably, frequency-aware methods like F³-Net [35] report limitations in cross-datasets adaptability. In contrast, our approach outperforms them by 9.5% AUC on Celeb-DF (v2), respectively. Compared to spatial-frequency fusion methods Two-branch [30] and SFDG [42], our method demonstrates improved robustness, justifying the effectiveness of the proposed hierarchical cross-modal fusion strategy in leveraging the complementary strengths of spatial and frequency features.

4.6 Ablation Study

In this section, we conduct ablation studies on our proposed key components – SCBM, SIDA, and HCMF – to systematically investigate their contributions to detection performance. Specifically, we sequentially remove each component and evaluate the corresponding AUC scores on FF++ (c23), with results detailed in Table 3.

Table 3: Results of ablation experiments on three key components: SCBM, HCMF and SIDA.

SCBM	HCMF	SIDA	AUC(%)
-	-	-	97.70
-	✓	✓	99.03
✓	-	✓	98.95
✓	✓	-	97.99
✓	✓	✓	99.58

Ablation Study on SCBM. SCBM is designed to capture subtle frequency-based forgery traces within individual image blocks. To evaluate its effectiveness, we removed SCBM from the local branch in the frequency domain while keeping all other modules unchanged, directly feeding the frequency-domain features into CNN-F. As shown in Table 3, this modification resulted in a 0.5% drop in performance, confirming SCBM’s ability to capture abrupt variations in DCT coefficients and enhance local spectral feature representation.

Ablation Study on Hierarchical Cross-Modal Fusion. The proposed hierarchical fusion framework consists of FAAE module and HCMA module, which jointly model and integrate spatial and multi-scale frequency-domain features. Replacing this mechanism with a simple concatenation of spatial and frequency features led to a 0.6% performance decrease, demonstrating the effectiveness of our design. Further ablation was conducted by individually removing the FAAE and HCMA modules. As shown in Table 4, the framework achieves optimal performance only when both modules are jointly employed, highlighting their complementary roles in enhancing cross-modal feature fusion.

Ablation Study on SIDA. The SIDA aims to fully leverage global frequency differential statistical characteristics. By removing the SIDA (Global Branch) in the frequency domain and retaining only

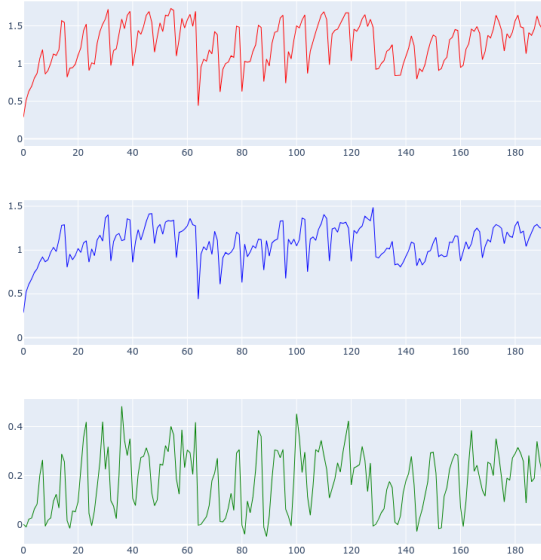


Figure 7: The line charts of the differential statistical metrics in SIDA. Red represents authentic faces, blue denotes forged faces, and green indicates the difference between them.

the hierarchical cross-modal fusion of spatial features and local frequency-domain features. As shown in Table 3, performance declined by 1.4%. This validates the effectiveness of the SIDA in feature refinement.

To provide a more intuitive visualization of SIDA’s effects, we plotted line charts (using the mean as an example and considering only the Y component) for the differential statistical metrics in SIDA. As shown in Figure 7, the 192-dimensional feature space consists of three segments: the first 64 dimensions correspond to inter-block row differences, the middle 64 dimensions represent inter-block column differences, and the last 64 dimensions indicate intra-block differences. The results demonstrate that SIDA effectively amplifies the distinctions between authentic and forged images in mid-to-high frequency ranges.

Table 4: Results of ablation experiments on key components (FAAE and HCMA) of HCMAF

FAAE	HCMA	AUC(%)
-	-	97.70
✓	-	98.30
-	✓	99.27
✓	✓	99.58

5 Conclusion

In this paper, we introduced a Spatial-Frequency Collaborative Learning framework with Hierarchical Cross-Modal Fusion for robust deepfake detection. First, a block-wise DCT analysis with

inter/intra-block multi-scale frequency-convolutional network was proposed to enhance local representation learning and enable precise forgery localization in the frequency domain. Second, a scale-invariant differential analysis approach was designed to capture holistic forgery traces while mitigating multi-scale discrepancies and post-processing interference. Finally, a hierarchical cross-modal fusion mechanism unified shallow-layer attention refinement and deep-layer dynamic modulation, addressing spatial-frequency interdependencies and feature heterogeneity across modalities. Extensive in-dataset and cross-dataset experiments demonstrate the superior detection performance and generalization capability of our method. Ablation studies further validate the critical role of the various key components in our design.

Acknowledgments

To Robert, for the bagels and explaining CMYK and color spaces.

References

- [1] Darius Afchar, Vincent Nozick, Junichi Yamagishi, and Isao Echizen. 2018. Mesonet: a compact facial video forgery detection network. In *2018 IEEE international workshop on information forensics and security (WIFS)*. IEEE, 1–7.
- [2] Aayushi Agarwal, Akshay Agarwal, Sayan Sinha, Mayank Vatsa, and Richa Singh. 2021. MD-CSDNetwork: Multi-domain cross stitched network for deepfake detection. In *2021 16th IEEE international conference on automatic face and gesture recognition (FG 2021)*. IEEE, 1–8.
- [3] Shruti Agarwal, Hany Farid, Ohad Fried, and Maneesh Agrawala. 2020. Detecting deep-fake videos from phoneme-viseme mismatches. In *Proceedings of the IEEE/CVF conference on computer vision and pattern recognition workshops*. 660–661.
- [4] Martin Arjovsky and Soumith Chintala. 2017. Bottou. wasserstein gan. *arXiv preprint arXiv:1701.07875* 7 (2017).
- [5] Zhongjie Ba, Qingyu Liu, Zhenguang Liu, Shuang Wu, Feng Lin, Li Lu, and Kui Ren. 2024. Exposing the deception: Uncovering more forgery clues for deepfake detection. In *Proceedings of the AAAI Conference on Artificial Intelligence*, Vol. 38. 719–728.
- [6] Zhongjie Ba, Qingyu Liu, Zhenguang Liu, Shuang Wu, Feng Lin, Li Lu, and Kui Ren. 2024. Exposing the deception: Uncovering more forgery clues for deepfake detection. In *Proceedings of the AAAI Conference on Artificial Intelligence*, Vol. 38. 719–728.
- [7] Yunjey Choi, Minje Choi, Munyoung Kim, Jung-Woo Ha, Sunghun Kim, and Jaegul Choo. 2018. Stargan: Unified generative adversarial networks for multi-domain image-to-image translation. In *Proceedings of the IEEE conference on computer vision and pattern recognition*. 8789–8797.
- [8] François Chollet. 2017. Xception: Deep learning with depthwise separable convolutions. In *Proceedings of the IEEE conference on computer vision and pattern recognition*. 1251–1258.
- [9] Umur Aybars Ciftci, Ilke Demir, and Lijun Yin. 2020. Fakecatcher: Detection of synthetic portrait videos using biological signals. *IEEE transactions on pattern analysis and machine intelligence* (2020).
- [10] Brian Dolhansky, Joanna Bitton, Ben Pfau, Jikuo Lu, Russ Howes, Menglin Wang, and Cristian Canton Ferrer. 2020. The deepfake detection challenge (dfdc) dataset. *arXiv preprint arXiv:2006.07397* (2020).
- [11] Shichao Dong, Jin Wang, Jiajun Liang, Haoqiang Fan, and Renhe Ji. 2022. Explaining deepfake detection by analysing image matching. In *European conference on computer vision*. Springer, 18–35.
- [12] Alexey Dosovitskiy, Lucas Beyer, Alexander Kolesnikov, Dirk Weissenborn, Xiuhua Zhai, Thomas Unterthiner, Mostafa Dehghani, Matthias Minderer, Georg Heigold, Sylvain Gelly, et al. 2020. An image is worth 16x16 words: Transformers for image recognition at scale. *arXiv preprint arXiv:2010.11929* (2020).
- [13] Ricard Durall, Margret Keuper, Franz-Josef Pfundt, and Janis Keuper. 2019. Unmasking deepfakes with simple features. *arXiv preprint arXiv:1911.00686* (2019).
- [14] Shuaijv Fang, Zhiyong Zhang, and Bin Song. 2025. Deepfake Detection Model Combining Texture Differences and Frequency Domain Information. *ACM Transactions on Privacy and Security* 28, 2 (2025), 1–16.
- [15] Steven Fernandes, Sunny Raj, Eddy Ortiz, Iustina Vintila, Margaret Salter, Gordana Urosevic, and Sumit Jha. 2019. Predicting heart rate variations of deepfake videos using neural ode. In *Proceedings of the IEEE/CVF international conference on computer vision workshops*. 0–0.
- [16] Qiqi Gu, Shen Chen, Taiping Yao, Yang Chen, Shouhong Ding, and Ran Yi. 2022. Exploiting fine-grained face forgery clues via progressive enhancement learning.

- In *Proceedings of the AAAI conference on artificial intelligence*, Vol. 36. 735–743.
- [17] Zhenliang He, Wangmeng Zuo, Meina Kan, Shiguang Shan, and Xilin Chen. 2019. Attgan: Facial attribute editing by only changing what you want. *IEEE transactions on image processing* 28, 11 (2019), 5464–5478.
 - [18] Javier Hernandez-Ortega, Ruben Tolosana, Julian Fierrez, and Aythami Morales. 2020. Deepfakeson-phys: Deepfakes detection based on heart rate estimation. *arXiv preprint arXiv:2010.00400* (2020).
 - [19] Tero Karras, Timo Aila, Samuli Laine, and Jaakko Lehtinen. 2017. Progressive growing of gans for improved quality, stability, and variation. *arXiv preprint arXiv:1710.10196* (2017).
 - [20] Tero Karras, Samuli Laine, and Timo Aila. 2019. A style-based generator architecture for generative adversarial networks. In *Proceedings of the IEEE/CVF conference on computer vision and pattern recognition*. 4401–4410.
 - [21] Jiaming Li, Hongtao Xie, Jiahong Li, Zhongyuan Wang, and Yongdong Zhang. 2021. Frequency-aware discriminative feature learning supervised by single-center loss for face forgery detection. In *Proceedings of the IEEE/CVF conference on computer vision and pattern recognition*. 6458–6467.
 - [22] Jiaming Li, Hongtao Xie, Lingyun Yu, and Yongdong Zhang. 2022. Wavelet-enhanced weakly supervised local feature learning for face forgery detection. In *Proceedings of the 30th ACM international conference on multimedia*. 1299–1308.
 - [23] Lingzhi Li, Jianmin Bao, Hao Yang, Dong Chen, and Fang Wen. 2019. Faceshifter: Towards high fidelity and occlusion aware face swapping. *arXiv preprint arXiv:1912.13457* (2019).
 - [24] Lingzhi Li, Jianmin Bao, Ting Zhang, Hao Yang, Dong Chen, Fang Wen, and Baining Guo. 2020. Face x-ray for more general face forgery detection. In *Proceedings of the IEEE/CVF conference on computer vision and pattern recognition*. 5001–5010.
 - [25] Yuezun Li, Xin Yang, Pu Sun, Honggang Qi, and Siwei Lyu. 2020. Celeb-df: A large-scale challenging dataset for deepfake forensics. In *Proceedings of the IEEE/CVF conference on computer vision and pattern recognition*. 3207–3216.
 - [26] Li Lin, Xinan He, Yan Ju, Xin Wang, Feng Ding, and Shu Hu. 2024. Preserving fairness generalization in deepfake detection. In *Proceedings of the IEEE/CVF Conference on Computer Vision and Pattern Recognition*. 16815–16825.
 - [27] Decheng Liu, Tao Chen, Chunlei Peng, Nannan Wang, Ruimin Hu, and Xinbo Gao. 2024. Attention Consistency Refined Masked Frequency Forgery Representation for Generalizing Face Forgery Detection. *IEEE Transactions on Information Forensics and Security* (2024).
 - [28] Honggu Liu, Xiaodan Li, Wenbo Zhou, Yuefeng Chen, Yuan He, Hui Xue, Weiming Zhang, and Nenghai Yu. 2021. Spatial-phase shallow learning: rethinking face forgery detection in frequency domain. In *Proceedings of the IEEE/CVF conference on computer vision and pattern recognition*. 772–781.
 - [29] Yuchen Luo, Yong Zhang, Junchi Yan, and Wei Liu. 2021. Generalizing face forgery detection with high-frequency features. In *Proceedings of the IEEE/CVF conference on computer vision and pattern recognition*. 16317–16326.
 - [30] Iacopo Masi, Aditya Killekar, Royston Marian Mascarenhas, Shenoy Pratik Gurudatt, and Wael AbdAlmageed. 2020. Two-branch recurrent network for isolating deepfakes in videos. In *Computer vision—ECCV 2020: 16th European conference, glasgow, UK, August 23–28, 2020, proceedings, part VII 16*. Springer, 667–684.
 - [31] Changtao Miao, Zichang Tan, Qi Chu, Nenghai Yu, and Guodong Guo. 2022. Hierarchical frequency-assisted interactive networks for face manipulation detection. *IEEE Transactions on Information Forensics and Security* 17 (2022), 3008–3021.
 - [32] Dat Nguyen, Nesryne Mejri, Inder Pal Singh, Polina Kuleshova, Marcella Astrid, Anis Kacem, Enjie Ghorbel, and Djamilia Aouada. 2024. Laa-net: Localized artifact attention network for quality-agnostic and generalizable deepfake detection. In *Proceedings of the IEEE/CVF Conference on Computer Vision and Pattern Recognition*. 17395–17405.
 - [33] Yuval Nirkin, Lior Wolf, Yosi Keller, and Tal Hassner. 2021. Deepfake detection based on discrepancies between faces and their context. *IEEE transactions on pattern analysis and machine intelligence* 44, 10 (2021), 6111–6121.
 - [34] Hua Qi, Qing Guo, Felix Juefei-Xu, Xiaofei Xie, Lei Ma, Wei Feng, Yang Liu, and Jianjun Zhao. 2020. Deephythm: Exposing deepfakes with attentional visual heartbeat rhythms. In *Proceedings of the 28th ACM international conference on multimedia*. 4318–4327.
 - [35] Yuyang Qian, Guojun Yin, Lu Sheng, Zixuan Chen, and Jing Shao. 2020. Thinking in frequency: Face forgery detection by mining frequency-aware clues. In *European conference on computer vision*. Springer, 86–103.
 - [36] Andreas Rossler, Davide Cozzolino, Luisa Verdoliva, Christian Riess, Justus Thies, and Matthias Nießner. 2019. Faceforensics++: Learning to detect manipulated facial images. In *Proceedings of the IEEE/CVF international conference on computer vision*. 1–11.
 - [37] Chuangchuan Tan, Yao Zhao, Shikui Wei, Guanghua Gu, Ping Liu, and Yunchao Wei. 2024. Frequency-aware deepfake detection: Improving generalizability through frequency space domain learning. In *Proceedings of the AAAI Conference on Artificial Intelligence*, Vol. 38. 5052–5060.
 - [38] Mingxing Tan and Quoc Le. 2019. Efficientnet: Rethinking model scaling for convolutional neural networks. In *International conference on machine learning*. PMLR, 6105–6114.
 - [39] Justus Thies, Michael Zollhofer, Marc Stamminger, Christian Theobalt, and Matthias Nießner. 2016. Face2face: Real-time face capture and reenactment of rgb videos. In *Proceedings of the IEEE conference on computer vision and pattern recognition*. 2387–2395.
 - [40] Junke Wang, Zuxuan Wu, Wenhao Ouyang, Xintong Han, Jingjing Chen, Yugang Jiang, and Ser-Nam Li. 2022. M2tr: Multi-modal multi-scale transformers for deepfake detection. In *Proceedings of the 2022 international conference on multimedia retrieval*. 615–623.
 - [41] Tianyi Wang and Kam Pui Chow. 2023. Noise based deepfake detection via multi-head relative-interaction. In *Proceedings of the AAAI Conference on Artificial Intelligence*, Vol. 37. 14548–14556.
 - [42] Yuan Wang, Kun Yu, Chen Chen, Xiyuan Hu, and Silong Peng. 2023. Dynamic graph learning with content-guided spatial-frequency relation reasoning for deepfake detection. In *Proceedings of the IEEE/CVF conference on computer vision and pattern recognition*. 7278–7287.
 - [43] Xi Wu, Zhen Xie, YuTao Gao, and Yu Xiao. 2020. Sstnet: Detecting manipulated faces through spatial, steganalysis and temporal features. In *ICASSP 2020-2020 IEEE international conference on acoustics, speech and signal processing (ICASSP)*. IEEE, 2952–2956.
 - [44] Kai Xu, Minghai Qin, Fei Sun, Yuhao Wang, Yen-Kuang Chen, and Fengbo Ren. 2020. Learning in the frequency domain. In *Proceedings of the IEEE/CVF conference on computer vision and pattern recognition*. 1740–1749.
 - [45] Xin Yang, Yuezun Li, and Siwei Lyu. 2019. Exposing deep fakes using inconsistent head poses. In *ICASSP 2019-2019 IEEE international conference on acoustics, speech and signal processing (ICASSP)*. IEEE, 8261–8265.
 - [46] Qilin Yin, Wei Lu, Bin Li, and Jiwu Huang. 2023. Dynamic difference learning with spatio-temporal correlation for deepfake video detection. *IEEE Transactions on Information Forensics and Security* 18 (2023), 4046–4058.
 - [47] Dengyong Zhang, Jiahao Chen, Xin Liao, Feng Li, Jiaxin Chen, and Gaobo Yang. 2024. Face forgery detection via multi-feature fusion and local enhancement. *IEEE Transactions on Circuits and Systems for Video Technology* (2024).
 - [48] Daichi Zhang, Fanzhao Lin, Yingying Hua, Pengju Wang, Dan Zeng, and Shiming Ge. 2022. Deepfake video detection with spatiotemporal dropout transformer. In *Proceedings of the 30th ACM international conference on multimedia*. 5833–5841.
 - [49] Hanqing Zhao, Wenbo Zhou, Dongdong Chen, Tianyi Wei, Weiming Zhang, and Nenghai Yu. 2021. Multi-attentional deepfake detection. In *Proceedings of the IEEE/CVF conference on computer vision and pattern recognition*. 2185–2194.
 - [50] Peng Zhou, Xintong Han, Vlad I Morariu, and Larry S Davis. 2017. Two-stream neural networks for tampered face detection. In *2017 IEEE conference on computer vision and pattern recognition workshops (CVPRW)*. IEEE, 1831–1839.